Technical University of Denmark

DTU

The influence of trailed vorticity on flutter speed estimations

Pirrung, Georg; Aagaard Madsen , Helge; Kim, Taeseong

[Link back to DTU Orbit]

DTU Library
Technical Information Center of Denmark

The influence of trailed vorticity on flutter speed estimations

Georg R. Pirrung, Helge Aa. Madsen and Taeseong Kim

DTU Wind Energy, Frederiksborgvej 399, Roskilde, DK

E-mail: `gepir@dtu.dk`

Abstract. This paper briefly describes the implementation of a coupled near and far wake model for wind turbine rotor induction in the aeroelastic code HAWC2 and its application for flutter analysis of the NREL 5 MW wind turbine. The model consists of a far wake part based on Blade Element Momentum (BEM) theory, which is coupled with Beddoes' near wake model for trailed vorticity.

The first part of this work outlines the implementation in HAWC2, with a focus on the interaction of the induction from the blade based near wake model with the induction from the polar grid based BEM model in HAWC2.

The influence of the near wake model on the aeroelastic stability of the blades of the NREL 5 MW turbine in overspeed conditions is investigated in the second part of the paper. The analysis is based on a runaway case in which the turbine is free to speed up without generator torque and vibrations start building up at a critical rotor speed. Blades with modified torsional and flapwise stiffness are also investigated. A flutter analysis is often part of the stability investigations for new blades but is normally carried out with engineering models that do not include the influence of unsteady trailed vorticity. Including this influence results in a slightly increased safety margin against classical flutter in all simulated cases.

1. Introduction

Most of the aeroelastic codes used in the wind turbine industry are based on Blade Element Momentum (BEM) theory to model the induced wind speeds due to the aerodynamic forces at the rotor disc, cf. [1]. The trailed vorticity, which depends on the radial gradient of the bound circulation along the blade, is in these codes only implicitly included for the tip vortex in form of a tip loss correction, but the dynamic effects of the trailed vorticity are neglected. Hansen [2] names these near wake effects as one of the state-of-the-art issues in predicting flutter limits for wind turbines. In this paper the influence of these effects on the critical rotor speeds, the rotor speeds where blade vibrations with negative damping start to build up, is investigated for the NREL 5MW reference turbine [3].

Flutter instabilities for large turbines have been investigated by for example Hansen [2, 4] and Lobitz [5, 6]. Both found that including the unsteady shed vorticity effects in the aerodynamic models led to increased flutter speeds and that the rotor speeds in normal operation are closer to critical rotor speeds for modern turbines with larger, more flexible blades than for small turbines. Thus a more accurate prediction of flutter speeds might become more important for future turbines.

This study uses the aeroelastic wind turbine code HAWC2 [7, 8, 9], in which a polar grid based

BEM model enables azimuth dependent induction, such as in sheared inflow [10]. To this BEM model a near wake model developed by Beddoes [11] and suggested for wind turbine application by Madsen and Rasmussen [12], has been added. The near wake model is a numerically efficient prescribed wake lifting line model, which allows for trailed vorticity computation without drastically slowing down the aeroelastic code. The motivation for the trailed vorticity modelling is to obtain a more precise dynamic induction prediction compared to a purely BEM based model and to remove the need for an additional tip loss correction. The dynamic induction due to the shed vorticity is modelled by the Beddoes Leishman dynamic stall model [13] in HAWC2, which includes the unsteady effects in the linear lift slope region. The near wake model needs to be stabilized in an iterative procedure and the possibility of accelerating the model by taking less important parts of the model out of the iteration loop is shown in this work.

The critical rotation speeds are obtained by simulating runaway cases, where the turbine is operating without generator torque and at a fixed pitch angle of zero. The rotor is thus free to speed up and the rotor speed can be controlled by the wind speed. To approach a critical rotor speed, the wind speed is accelerated following a slow ramp. The influence of the wind speed gradient in that ramp is briefly investigated in this paper. The structural stiffnesses of the NREL 5MW blade regarding both flapwise bending and torsion are modified to show the influence of the near wake model for different blades.

The next section gives a brief description of the grid-based BEM HAWC2 model, followed by the implementation of the near wake model. Then the runaway cases and a simple method to approximate the mode shapes of the unstable vibrations in HAWC2 is explained. Finally, critical flutter speeds comparing the original HAWC2 model with the extended HAWC2 model including the near wake model, in the following denoted as HAWC2 NW, are presented.

2. Implementation of a near wake model in the aeroelastic code HAWC2
2.1. BEM in HAWC2
The classic BEM method divides the rotor disc into annular elements, where the quasi steady induction is calculated based on the local thrust at each radial section. To enable different inductions at different parts of the rotor disc, e.g. top and bottom in case of wind shear, the annular elements are in HAWC2 divided by azimuthal sections, leading to a non-rotating polar grid. Two first order filters with time constants depending on the loading and the radial position are applied on the quasi steady induction at each grid point to include the dynamic inflow effect. The grid-based computation of the induction is described by Madsen et al. in [10].

The induction and free wind speed, stored on the polar grid, are needed to compute the flow and resulting forces at the blades and the blade velocity and pitch angle are needed to compute the thrust coefficient on the grid. Azimuthal interpolation is therefore necessary both from the closest grid points to the blade and from the closest blades to the grid point.

2.2. Implementation of the near wake model in the HAWC2 aerodynamic model
The near wake model is used to compute the induction due to the trailed vorticity in a quarter rotation behind the blades. Vorticity is trailed from vortex trailing points at the root and tip of the blade, as well as between the aerodynamic sections that are used to compute the local forces on the blade. Each blade is only influenced by induction due to its own trailed vorticity.

In principle, the induction at each radial position on the blade would be computed as the result of a numerical integral of the Biot-Savart law over the trailed vortex elements, each at the length of one time step, behind the blade. Beddoes, [11], proposed to approximate the decreasing induction due to a vortex element as it moves away from the blade by two exponential functions. This approximation makes it possible to increase the computation speed, because the influence of all previously trailed elements decreases by the same factor in a time step. To obtain the induction in a following timestep, it is therefore sufficient to multiply the total induction of all

previously trailed elements by this factor and add the contribution from the newest element trailed in the time step.

In the original form, the near wake model assumed the trailed vorticity to stay in the rotor plane, but in this paper a correction for downwind convection is included in the model. With this correction the vorticity moves along helical paths, where the pitch angle of the helix depends on the local flow at the respective radial blade section.

Because the near wake model gives the induction at the blade position due to the vorticity trailed from the respective blade, the induced velocity from the near wake is in HAWC2 treated in the same way as blade velocity and pitch angle, that is as a local blade parameter. This means that the total induction is consisting of one part that is computed in the fixed polar grid, the far wake induction, and one part that is rotating with the blades, the near wake induction. To obtain the far wake induction, the BEM induction is scaled by a coupling factor that is smaller than one. The coupling factor is determined so that the integral thrust force of HAWC2 NW matches the HAWC2 BEM model with tip loss correction. The near wake model needs to be iterated to ensure a stable operation. One call of the aerodynamic model HAWC2 NW is structured as follows:

(i) BEM induction

   (a) Find the two closest blades to each grid point

   (b) Calculate thrust coefficient using blade velocity, pitch angles and near wake induction of each of the two closest blades

   (c) Interpolate thrust coefficient at the grid point based on azimuth angle

   (d) Calculate far wake induction

(ii) Near wake induction

   (a) Find closest grid points to each blade section

   (b) Interpolate far wake induction and wind speed

   (c) Iterate until convergence:

      1. Compute angles of attack and relative velocity

      2. Compute length and helix pitch angle of trailed vorticity

      3. Compute quasi-steady circulation at each blade section

      4. Apply time lags to account for dynamic circulation buildup

      5. Compute induction from trailed vorticity in the near wake

      6. Apply relaxation factor on near wake induction

(iii) Calculate dynamic lift, drag and moment coefficients, using the dynamic stall model in [13]. These coefficients do not feed back back to the BEM induction, but are used to determine the forces on the structure.

3. Flutter speed prediction scheme

In this section, the flutter speed prediction scheme used in this work is described, together with the method used to extract the mode shapes of negatively damped vibrations from HAWC2 simulations.

3.1. Run away case

To find a critical speed at which an aeroelastic turbine mode becomes negatively damped, the turbine has been simulated in a runaway situation, where the generator torque and pitch angle are zero. The rotor will in this case approach a rotation speed where the aerodynamic torque is zero, due to negative torque from the outer part of the blade and positive torque from the in board sections. This terminal rotor speed depends only on the wind speed at the rotor. To approach the critical rotor speed where an instability occurs the wind speed can be slowly ramped up, thus continuously increasing the rotor speed until vibrations of the blades start to

build up, cf. Figure 1. In general there is no disturbance other than numerical errors to start the vibration. In Section 4.1 the influence of turbulence as additional excitation on the flutter speed is evaluated.

Advantages of this approach compared to for example prescribing an increasing rotor speed through the generator torque at a fixed wind speed are:

- The runaway case is a better approximation of an overspeed situation because no artificial forcing is necessary.
- The edgewise blade deflections are small because the rotor torque is close to zero. Edgewise deflection will change the coupling between flapwise, edgewise and torsional blade modes and change the flutter speed, in the same way as sweeping the blades would [14].
- The influence of the wind speed slope, which is the only relevant parameter for the simulation, is small, cf. Results section.

In all observed cases, the instability will, since the rotor speed is free to change, first lead to small oscillations of the rotor speed and then to a significant decrease of the rotor speed, as energy from the rotation is transferred to vibrations of the blades. In the following flutter speed comparisons, the flutter speed has been determined at the time where the rotation speed in one time step is smaller than in the previous time step for the first time in the simulation except the transients at the start up, cf. Figure 2.

3.2. Mode shape extraction
To compare the unstable blade vibrations obtained in the HAWC2, a simple routine has been developed. It requires output of the time series of edgewise and flapwise deflection as well as torsion along the blade. The algorithm fits a cosine function, $g = a \cos(ft - \phi)$, with the variables amplitude a, frequency f and phase ϕ, to a short, moving window of 0.5 seconds of the time series of the flapwise tip deflection, minimizing the error of the cosine fit with the original time series data. When a flapwise amplitude of $a = 0.1m$ is found in a time window, the algorithm extracts the mode shape by fitting cosine functions to deflections and rotations at all available radial stations of the blade. The amplitude of $0.1m$ was chosen because it proved to be a good compromise between extracting the small vibrations at the start of the instability and having large enough amplitudes along the blade to ensure a good performance of the curve fitting algorithm. In this way, the radial distributions of both amplitudes and phases of the
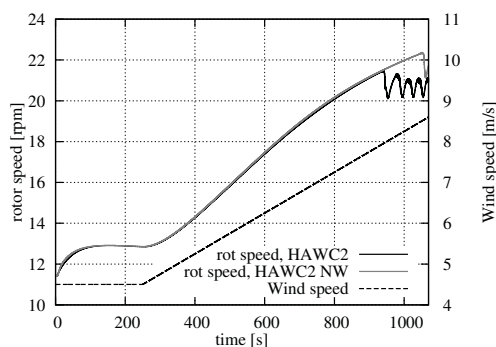

Figure 1. Principle of the runaway case: the wind speed is slowly ramped up and the rotor speed follows up to an instability. Comparison between HAWC2 with BEM and coupled near and far wake model.
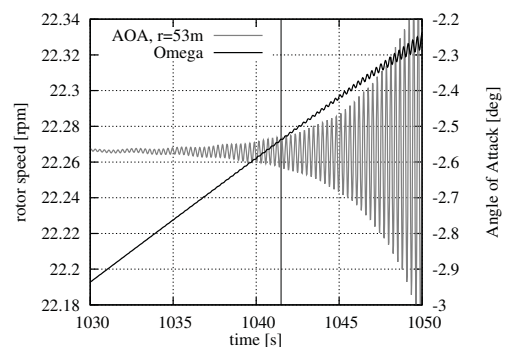
Figure 2. Zoom to the onset of vibrations. The black vertical line indicates the time interpreted here as the onset of flutter.

components of the blade vibration can be determined, leading to something similar to a mode shape. Because HAWC2 is able to capture the structural nonlinearities due to large deflections, the deflection shapes will vary with amplitude, so they are not equivalent to mode shapes in linear vibration theory. Still, they can be used to qualitatively compare the different instabilities obtained with the HAWC2 and HAWC2 NW models.

4. Results
In this section, flutter speeds of the NREL 5 MW turbine [3] and modified versions with stiffer and softer blades computed with HAWC2 and HAWC2 NW are compared. In all simulations the twist and cone of the turbine has been set to zero and there is no wind shear, yaw error and gravity. In the last part of the section the mode shapes of some of the observed vibrations are compared to obtain further insight in the effects of the trailed vorticity.

4.1. Sensitivity to ramping speed and disturbance
Figure 3 shows the sensitivity of the Flutter speeds predicted using the HAWC2 and HAWC2 NW models to changes in ramping speed. It can be seen that over the range of ramping speeds the flutter speeds are changing only slightly, by about 3% if the near wake model is included and 5% if the traditional HAWC2 BEM model is used. Note that this small change in flutter speed is a consequence of changing the ramping speed by a factor of 16 from 0.00125 m/s^2 to 0.02 m/s^2. The predicted flutter speeds are higher for faster ramping speed, which might be partially because the instabilities need some time to build up. At faster ramping speeds the rotor accelerates faster, leading to a bigger increase in rotor speed between the first small blade oscillations and a decrease in rotor speed that is used here to mark the onset of the instability. Because the difference between HAWC2 and HAWC2 NW results is similar for different ramping speeds and slow ramps require long computations, all further computations have been performed using a wind ramp with a slope of 0.005 m/s^2.

In Figure 4 the influence of added turbulence is shown for low turbulence intensities. Turbulence decreases the flutter speed when the original HAWC2 model is used, but has almost no influence in case of the near wake model. In Section 4.3 it is shown that the reason for this difference is that two different modes can become unstable in HAWC2 at slightly different relative speeds if the standard blade is used. It seems that the mode that becomes unstable at lower wind speeds, which is different than the mode observed in HAWC2 NW, cf. Section 4.3, is more affected by turbulence than the other mode. Even though there is a clear influence of turbulence intensity on the offset between the flutter speeds predicted by the near wake model and the original HAWC2 model in this particular case, it has been decided to run all following computations without turbulence to avoid introducing an additional parameter.

4.2. Sensitivity to structural stiffness variations of the blade
Figure 5 shows the influence of the variation of both flapwise stiffness and torsional stiffness on the flutter speed. The cross section parameters Ix, the flapwise area moment of inertia, and Ip the torsional stiffness constant, have been artificially varied from 70 to 130 % of the original values for the NREL 5 MW turbine, keeping all other parameters constant. Both models agree that an increase of torsional blade stiffness leads to an increased stability, as expected. The flutter speed increase due to increased torsional stiffness is comparable in both models.

The flapwise stiffness variation, however, leads to different results. In agreement with findings by Lobitz [6], the flapwise stiffness has a smaller influence on the flutter speed than the torsional stiffness. In the present work, the direction in which an increasing flapwise stiffness changes the flutter speed is found to depend on both the blade and the used aerodynamic model: For the blade with 130% torsional stiffness, both aerodynamics models agree on a reduced flutter speed for increasing the flapwise stiffness from 100% to 130%. The most interesting behavior can
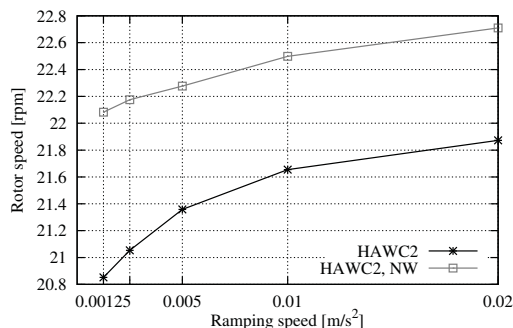
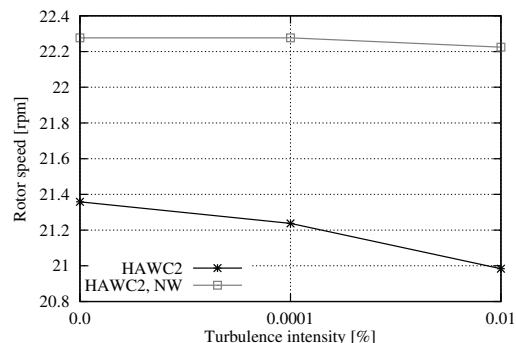**Figure 3.** Sensitivity of flutter speed with respect to ramping speed.

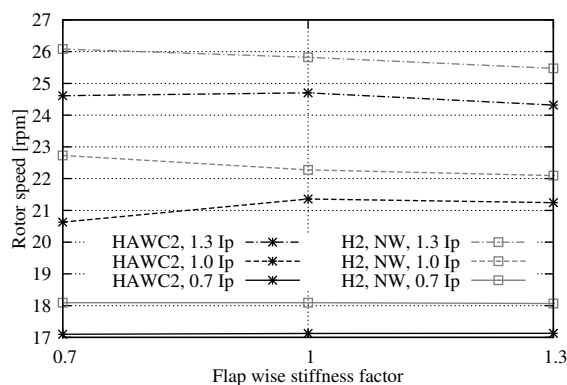**Figure 4.** Sensitivity of flutter speed with respect to turbulence intensity.

Figure 5. Sensitivity of flutter speed with respect to torsional and flapwise stiffness variations.

be seen when the flapwise stiffness is decreased from 100% to 70% for the otherwise unaltered blade. In this case the HAWC2 predicts a decrease in flutter speed, while HAWC2 NW shows an increased flutter speed. This case is further investigated in the next section based on the mode shapes of the vibrations simulated in HAWC2.

4.3. Vibration modes
The amplitudes and phases of deflections, axial induced velocity and aerodynamic forces of the blade vibrations are shown in Figures 6 and 7 for the cases with 70% and 130% flapwise stiffness and standard torsional stiffness. All amplitudes are normed by the flapwise tip amplitude and the plots show the mode shapes at a flapwise tip amplitude of 0.1 m. The phases are relative to the phase of the flapwise tip vibrations.

It can be seen that the vibrations of the softer blade, cf. Figure 6, agree well in the flapwise and torsional contents, but the HAWC2 computation predicts a much larger edgewise amplitude. In fact, the blade vibrates in different modes depending on the aerodynamic model; HAWC2 predicts a backward whirling mode with blade vibrations at 2.8 Hz, HAWC2 NW a symmetric flutter mode at 3.6 Hz. The frequency difference explains the different amplitudes of the aerodynamic forces, where HAWC2 NW predicts larger amplitudes even though the induction is responding much faster according to the near wake model.

In case of the stiffer blade, cf. Figure 7, both aerodynamic models predict the same unstable mode, a symmetric flutter mode at a frequency of 3.7 Hz. Magnitudes and phases of deflections and forces agree well between HAWC2 and HAWC2 NW, but the induced velocity is again
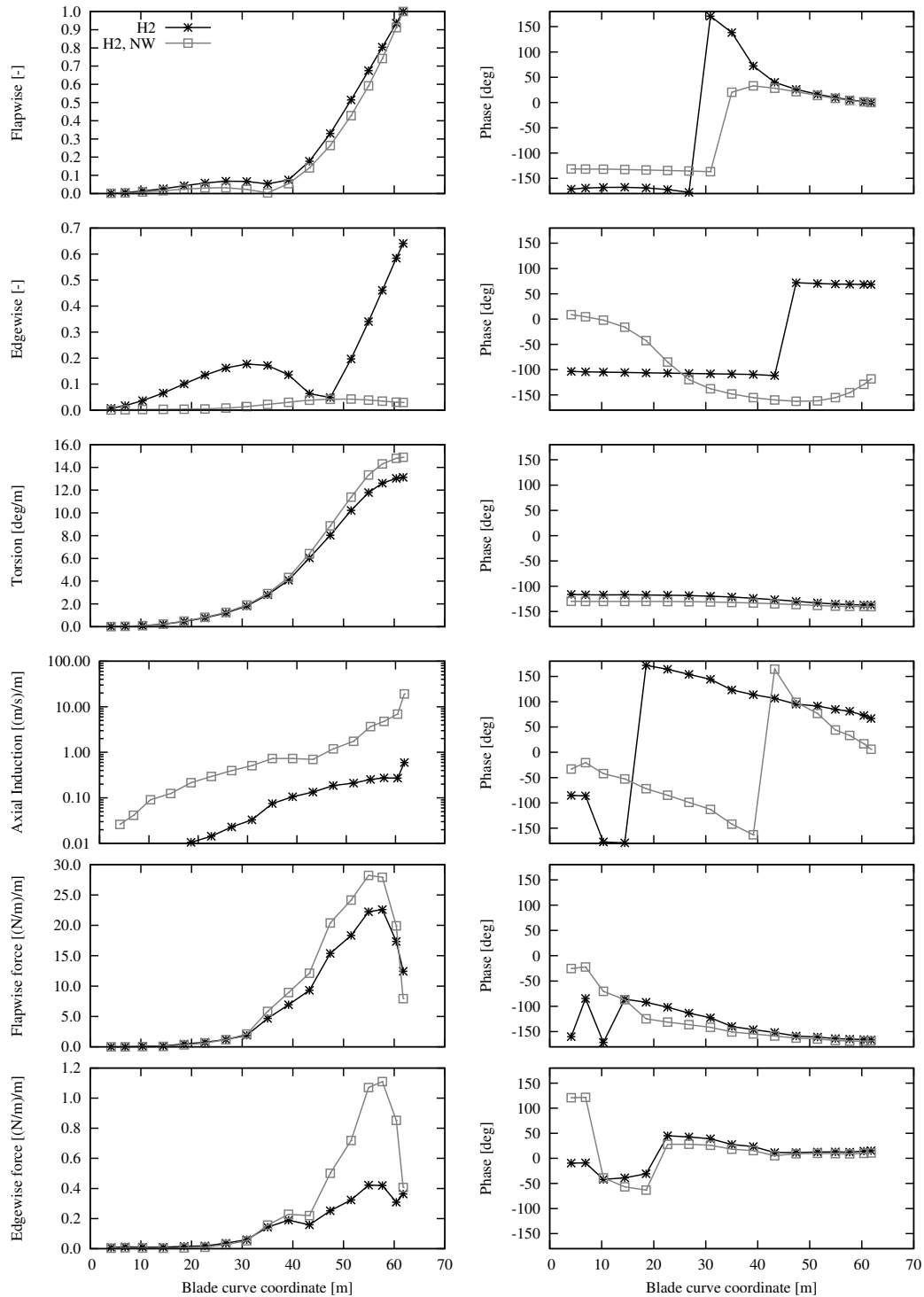
Figure 6. Comparison of unstable mode shapes of the turbine with blades at 70% stiffness, including the amplitudes and phases of induced velocity and aerodynamic forces. Different modes become unstable. The original HAWC2 model shows a backward whirling mode at a blade frequency of 2.8 Hz, the HAWC2 NW model a symmetric mode at 3.6 Hz.
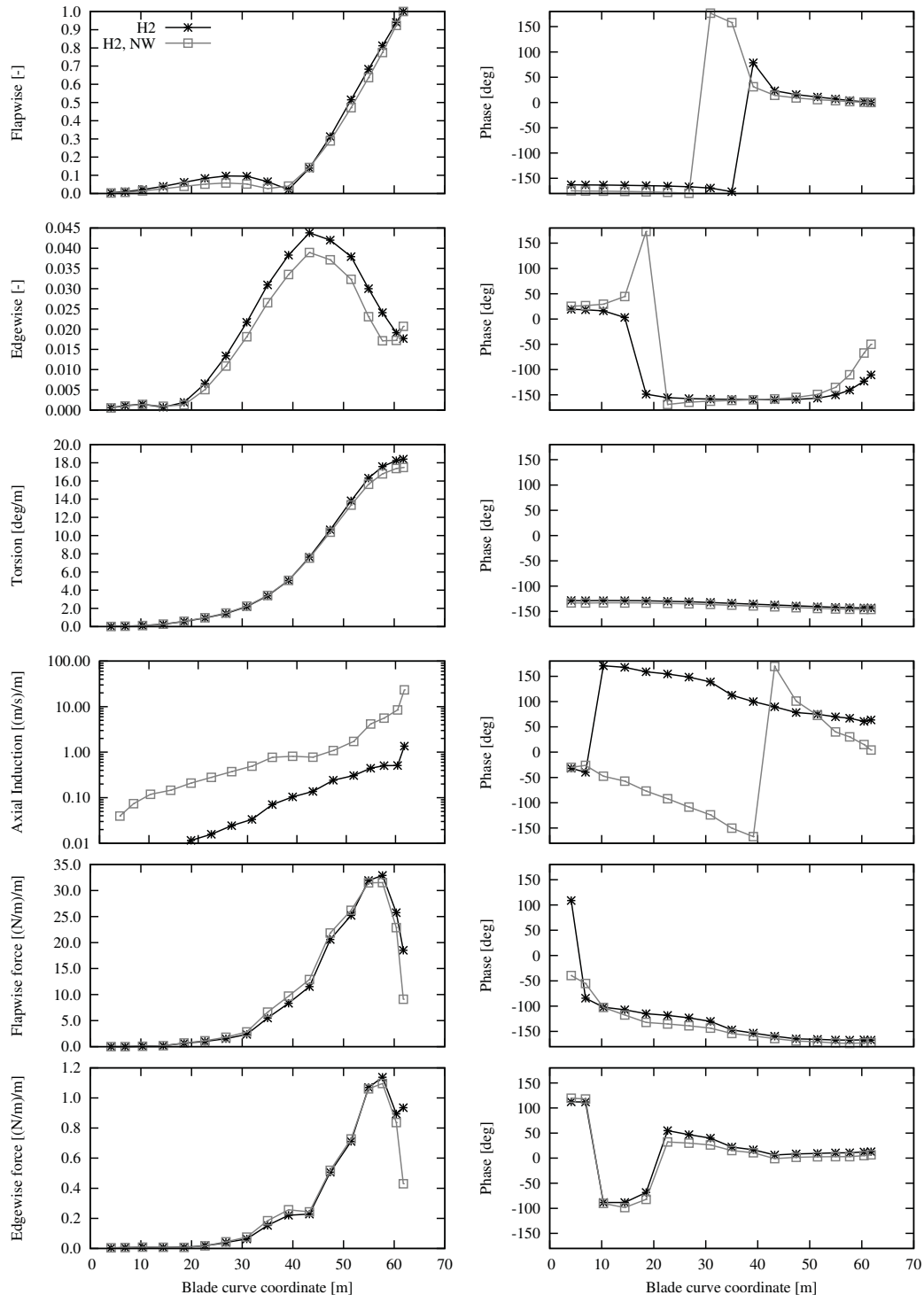
Figure 7. Comparison of unstable mode shapes of the turbine with blades at 70% stiffness, including the amplitudes and phases of induced velocity and aerodynamic forces. HAWC2 and HAWC2 NW agree on a symmetric mode with a very small edgewise component, at a frequency of 3.7 Hz. The large difference in induced velocity only has a small impact on the mode shape and the amplitudes and phases of aerodynamic forces.
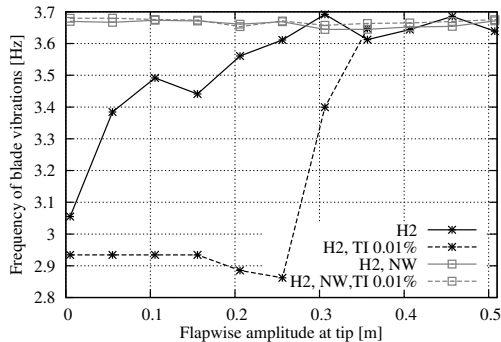
Figure 8. A shift of frequency can be observed on the standard NREL 5MW blade with the original HAWC2 aerodynamic model as the vibrations build up. Turbulence has a larger influence if the HAWC2 aerodynamic model is used.
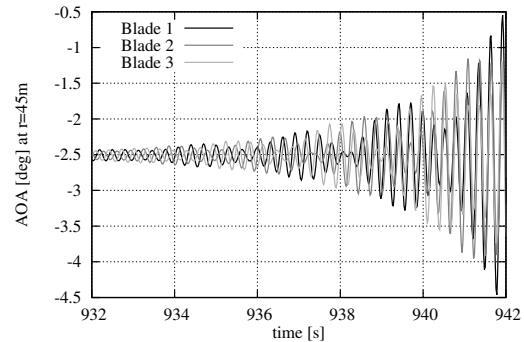

Figure 9. Time series of the AOA on the blades in the undisturbed case. At the onset of vibration, there is a 120 degree phase shift between blades, indicating a whirling mode. At small amplitudes, the vibrations start to synchronize.

computed with a larger amplitude by the near wake model.

The standard NREL 5MW blade with 100% flapwise and torsional stiffness exhibits an interesting behavior: if the original HAWC2 model is used, the frequency shifts from roughly 3.05 Hz at a very low flapwise amplitude of 5 mm to 3.65 Hz as the amplitude is increasing in the undisturbed case, cf. Figure 8. If turbulence is added to the HAWC2 computation, the vibrations start at lower rotation speed, cf. Figure 4, and stay at the low frequency also at higher amplitudes. An explanation for this behavior is that the whirling mode at the lower frequency might have a negative aeroelastic damping closer to zero than the symmetric mode. If that is the case, disturbance has a larger effect on the vibration buildup in the whirling mode because vibrations in the symmetric mode are growing faster starting from the very small numerical disturbance that is present in all the simulations.

Figure 9 shows in the time domain how the vibrations of the three different blades start out with a phase shift and synchronize during a short time in the undisturbed case. A comparison of the mode shapes predicted by HAWC2 and HAWC2 NW at small amplitude leads to a similar result as for the softer blade, cf. Figure 6, and at higher amplitudes the comparison is similar to the stiffer blade, cf. Figure 7, but the respective plots are not included in this paper for brevity.

A possible explanation for these findings is: the NREL 5 MW turbine can vibrate in overspeed in two modes with similar flapwise and torsional content, both in amplitude and phase. Depending on the aerodynamic model and the flapwise stiffness, either a backward whirling mode or a symmetric mode has a lower critical speed where the aeroelastic damping becomes negative. The trailed vorticity increases the critical speed of the whirling mode more than the critical speed of the symmetric mode, so that vibrations in the whirling mode are not observed in HAWC2 NW. In HAWC2, the whirling mode becomes unstable at lower rotation speed than the symmetric mode in case of the blade with reduced flapwise stiffness. This softer blade vibrates consistently in different modes depending on the aerodynamic model, which explains the larger difference in flutter speeds.

In case of the standard blade, the whirling mode seems to be unstable only at a small range of rotation speed and the observed vibrations quickly shift to the symmetric mode as the rotor accelerates. The stiffer blade vibrates in the same mode shape in the HAWC2 and HAWC2 NW computations, which may be a reason for the smaller difference in flutter speed predictions. This might only be a partial explanation of the observed phenomena, and further investigations are necessary for a more complete understanding.

5. Conclusions

The near wake model, originally developed by Beddoes, is implemented in the aeroelastic wind turbine code HAWC2. It is used to investigate the influence of trailed vorticity on the critical rotor speeds of the NREL 5 MW reference turbine with the original and modified blades, respectively. The critical rotor speeds are found by means of runaway cases, where the rotor is free to speed up at zero pitch angle and no generator torque.

It is shown that the critical rotor speed is almost independent of the slope of the wind speed ramp in the runaway cases. Including the trailed vorticity in the HAWC2 aerodynamic model has only slowed down the computation speed by a few percent. HAWC2 shows some dependence of the flutter speed on inflow turbulence, which can not be seen if the near wake model is used in the calculations.

The models agree that a torsional stiffness increase leads to an increase in flutter speeds. The influence of flapwise stiffness variations is smaller and less consistent. In some cases, the models disagree if an increased flapwise stiffness has a stabilizing or destabilizing effect.

More detailed investigations have shown that two different full turbine modes can be critical if the original torsional stiffness of the blade is used: a backward whirling mode and a symmetric mode. In near wake model computations only the symmetric mode can be observed. In case of the original HAWC2 model which of the two modes is critical depends on the flapwise blade stiffness. Further research is needed to understand in detail how the trailed vorticity stabilizes both modes.

In all cases investigated, the trailed vorticity in the near wake has a stabilizing effect and increases the flutter limit by roughly four to ten percent.

References

[1] Madsen H A, Riziotis V, Zahle F, Hansen M O L, Snel H, Grasso F, Larsen T J, Politis E and Rasmussen F 2012 Blade element momentum modeling of inflow with shear in comparison with advanced model results *Wind Energy* **15** 63–81

[2] Hansen M H 2007 Aeroelastic instability problems for wind turbines *Wind Energy* **10** 551–577

[3] Jonkman J, Butterfield S, Musial W and Scott G 2009 Definition of a 5-mw reference wind turbine for offshore system development Tech. rep. National Renewable Energy Laboratory

[4] Hansen M H and Madsen H A 2000 *Analyse af risikoen for flutter på vindmøllevinger* Denmark. Forskningscenter Risoe. Risoe-R-1196

[5] Lobitz D W 2004 Aeroelastic stability predictions for a MW-sized blade *Wind Energy* **7** 211–224

[6] Lobitz D W 2005 Parameter sensitivities affecting the flutter speed of a MW-sized blade *Journal of Solar Energy Engineering, Transactions of the ASME* **127** 538–543

[7] Larsen T and Hansen A 2007 *How 2 HAWC2, the user's manual* Denmark. Forskningscenter Risoe. Risoe-R-1597 ISBN 978-87-550-3583-6

[8] Kim T, Hansen A M and Branner K 2013 Development of an anisotropic beam finite element for composite wind turbine blades in multibody system *Renewable Energy* **59** 172 ISSN 09601481, 18790682

[9] Larsen T J, Madsen H A, Larsen G C and Hansen K S 2013 Validation of the dynamic wake meander model for loads and power production in the egmond aan zee wind farm *Wind Energy* **16** 605–624 ISSN 10954244, 10991824

[10] Madsen Aagaard H, Mikkelsen R, Sørensen N, Hansen M, Øye S and Johansen J 2007 *Influence of wind shear on rotor aerodynamics, power and loads* pp 101–116 Denmark. Forskningscenter Risoe. Risoe-R-1611 ISBN 978-87-550-3610-9

[11] Beddoes T S 1987 A near wake dynamic model *proc. of the AHS national specialist meeting on aerodynamics and aeroacoustics*

[12] Madsen H A and Rasmussen F 2004 A near wake model for trailing vorticity compared with the blade element momentum theory *Wind Energy* **7** 325–341

[13] Hansen M H, Gaunaa M and Madsen H A 2004 *A Beddoes-Leishman type dynamic stall model in state-space and indicial formulations* (Roskilde, Denmark: Risø-R-1354)

[14] Hansen M H 2011 *Aeroelastic properties of backward swept blades* Proceedings of 49th AIAA Aerospace Sciences Meeting Including The New Horizons Forum and Aerospace Exposition, Orlando